

#### ARTICLE INFO

Article ID: 02-13-02-0006 © 2020 SAE International doi:10.4271/02-13-02-0006

# Experimental Study of Tread Rubber Compound Effects on Tire Performance on Ice

Hoda Mousavi<sup>1</sup> and Corina Sandu<sup>1</sup>

<sup>1</sup>Virginia Tech, USA

### **Abstract**

Mechanical and thermal properties of the rubber compounds of a tire play an important role in the overall performance of the tire when it is in contact with the terrain. Although there are many studies conducted on the properties of the rubber compounds of the tire to improve some of the tire characteristics, such as the wear of the tread, there are a limited number of studies that focused on the performance of the tire when it is in contact with ice. This study is a part of a more comprehensive project looking into the tire-ice performance and modeling.

In this study, to understand the effect of different rubber compounds on the tire performance, three identical tires from the same company have been chosen. The tires' only difference is the material properties of the rubber. Two approaches have been implemented in this study. For the first approach, several tests were conducted for the chosen tires at Terramechanics, Multibody, and Vehicle Systems (TMVS) laboratory at Virginia Tech to compare their performance experimentally. For the second approach, a tire-ice model has been used to compute the height of the water film created at the contact patch. As will be shown in this study, an increase in the height of water film results in a decrease in the friction coefficient, which is one of the most critical parameters for the tire performance. By having this knowledge, the performance of the three tires considered in the study was compared using the developed tire-ice model, based on the values obtained for the height of the water film. It is shown that the results obtained by simulation coincide with the results obtained experimentally. The results from this study show the sensitivity of the magnitude of the tractive force with respect to parameters such as tire temperature, normal load, etc. The results also indicate that the tire with the lowest value of Young's modulus has the highest traction among all three tires used in this study.

#### **History**

Received: 10 Feb 2020 Revised: 27 Mar 2020 Accepted: 01 Jun 2020 e-Available: 16 Jun 2020

#### **Keywords**

Tire-ice modeling, Experimental method, Friction coefficient, Height of water film, Rubber compounds, Material properties of tread, Tire testing, Viscous friction, Slip ratio, Tire performance

#### Citation

Mousavi, H. and Sandu, C., "Experimental Study of Tread Rubber Compound Effects on Tire Performance on Ice," *SAE Int. J. Commer. Veh.* 13(2):89-101, 2020, doi:10.4271/02-13-02-0006.

ISSN: 1946-391X e-ISSN: 1946-3928

This article is based on and revised or modified from a presentation at WCX20, Detroit, MI, April 20-23, 2020 [2020-01-1228].







### 1. Introduction

everal research studies have been conducted on the areas related to tire interaction with different types of road and also the compounds and materials that can be used in the tire structure for more than a century [1, 2, 3, 4, 5, 6, 7, 8, 9, 10]. Considering the important effects of the tire tractive force on the vehicle control and stability, several past research studies used experimental or modeling approaches [11, 12] to investigate the effect of different parameters that influence the tire-road forces and moments. Among these studies, a limited number consider the road as an icy terrain and focus on the friction force of the tire [13]. In a study by Ivanovic et al. [14] investigating the rubber-ice friction dynamics, a comprehensive experimental study has been conducted. In this study, the effect of parameters such as vehicle speed and tire forces has been investigated.

In another study by Makkonen and Tikanmäki [15], it has been shown that the friction at the tire-ice contact area can be considered as dry friction for very low speed of the vehicle or very cold temperature of the ice. However, for higher speed, or temperature close to the melting temperature point of the ice, the heat generated by friction force may produce a water film on the top of the ice. The water film generated will change the nature of the friction force from completely dry friction to a combination of viscous and dry friction. The height of the water film created depends on several parameters, such as the ambient temperature, the ice temperature, the slip ratio, and the rubber compounds of the tire. Giessler et al. [16] performed an experimental study to investigate the effect of ambient temperature on tire-ice interaction. It has been shown that by increasing the ambient temperature the water film created increases.

The height of the water film created in the contact patch plays an important role in the magnitude of the viscous friction coefficient. Wiese et al. [17] developed a theoretical model to estimate the viscous friction coefficient for a sample rubber block in contact with ice using the water film generated in the contact patch. In this study, it has been shown that rubber samples with different compounds show different results when they are in contact with ice. In a study by Roberts [18], the influence of tread compounds on tire friction has been investigated. In this study, the effect of the glass transition temperature for the tire in contact with ice at different temperatures has been studied.

In this study, the main objective is the investigation on the effect of different tire-ice parameters, such as ice temperature and the material properties of the tread, on tire performance. For the experimental part of this study, several tests have been conducted for three tires with different rubber compounds. To understand the effect of each parameter on the tire friction forces, the results for each combination in the design of experiment (DOE) considered for this study have been presented and compared.

In addition to the experimental study, the height of the water film for each tire has been calculated using the developed Advanced Tire-Ice Interface Model (ATIIM2.0).

Considering the effect of this parameter on the tire-ice friction coefficient, investigating the results obtained for the height of the water film using simulation helped to compare the performance of the chosen tires.

This article includes seven sections. After a brief introduction in Section 1, Section 2 presents the input data for the material properties of the selected tires. Section 3 covers some general information about the Terramechanics Rig and also describes the testing procedure selected for this study. In Section 4, the DOE for this study is presented. The results from the experimental study are presented in Section 5. Section 6 includes the results obtained by the tire-ice model ATIIM2.0. A brief summary of the obtained results and the conclusions of the study are presented in Section 7.

# 2. Material Properties of the Selected Tires

To fulfill the main objective of this study (that is studying the effects of rubber compounds on tire performance on ice), three tires were chosen. Tires B, C, and G are all manufactured by the same company and are identical in tire dimensions and also tread pattern. Figure 1 shows the tread pattern of the chosen tires. The tires are only different in terms of the material properties of their tread. The tires are 205/55R1691Q with a width of 205 mm.

<u>Tables 1</u> and <u>2</u> show the thermal and mechanical material properties of each tire tested.

Where *E'* and *E''* are the storage and loss modulus, TAN-D is the phase angle and has been defined as the ratio of *E''* to *E'* and is called damping, and *E\** is the maximum stress over maximum strain [19]. According to the data given by Sumitomo, the density of the tread section of the Tires B, C, and G are 1,103 kg/m³, 1,094 kg/m³, and 1,137 kg/m³, respectively. These values are relatively close to each other. Furthermore, although outside the scope of this article, our research on these tires indicates that the rubber tread density slightly affects the viscous tire friction. As can be seen from

**FIGURE 1** Tread pattern of Tires B, C, and G used in this study.



AE Internationa

**TABLE 1** Specific heat values for Tires B, C, and G at different temperatures.

|                   | Temperature |      |      |      |  |  |
|-------------------|-------------|------|------|------|--|--|
|                   | [°C]        | В    | С    | G    |  |  |
|                   | -5          | 1.84 | 2.03 | 2.09 |  |  |
|                   | 0           | 1.88 | 2.14 | 2.26 |  |  |
|                   | 5           | 1.92 | 2.18 | 2.29 |  |  |
|                   | 10          | 1.94 | 2.21 | 2.31 |  |  |
|                   | 15          | 1.96 | 2.23 | 2.34 |  |  |
|                   | 20          | 1.99 | 2.26 | 2.36 |  |  |
|                   | 25          | 2.02 | 2.29 | 2.39 |  |  |
|                   | 30          | 2.05 | 2.32 | 2.42 |  |  |
|                   | 35          | 2.07 | 2.35 | 2.45 |  |  |
|                   | 40          | 2.09 | 2.37 | 2.47 |  |  |
|                   | 45          | 2.11 | 2.39 | 2.49 |  |  |
|                   | 50          | 2.12 | 2.40 | 2.51 |  |  |
|                   | 55          | 2.13 | 2.42 | 2.52 |  |  |
|                   | 60          | 2.16 | 2.44 | 2.54 |  |  |
| tiona             | 65          | 2.18 | 2.46 | 2.56 |  |  |
| SAE International | 70          | 2.20 | 2.49 | 2.59 |  |  |
| in In             | 75          | 2.23 | 2.52 | 2.62 |  |  |
| SA                | 80          | 2.26 | 2.55 | 2.65 |  |  |

 $\underline{\text{Tables 1}}$  and  $\underline{\text{2}}$ , Tire B has the lowest value of both, Young's modulus and the specific heat, compared with the other two tires.

To study the performance of each tire on ice, several tests were conducted under different operational conditions: traction performance for different slip ratios (from 2% to 30%), free-rolling condition, and also the braking condition for two levels of normal load (4 and 5.6 kN) and two levels of inflation pressure (144.8 and 193 kPa), in accordance with the DOE presented in the next section. The inflation pressure has been measured using a digital pressure gauge with a resolution of 0.5 psi. There were minimal differences in the ambient conditions in the lab during testing (in terms of temperature and moisture).

## 3. Design of Experiment

Table 3 shows the DOE implemented for this study. As it was mentioned, all three of the chosen tires are completely identical in all tire parameters except in their rubber compounds. Thus, in this study, the variables are material properties of the tread, applied normal load, inflation pressure of the tire, percentage of slip ratio, and temperature of the ice and tire. Although the ambient temperature was not the desired variable in this study, as it was not possible to conduct all the tests on the same day, this parameter was also measured and has been presented for each case of DOE. During all the tests, the camber and toe angles were equal to zero. However, the flexible design of the rig gives us the opportunity of performing

**TABLE 2** Young's modulus values for Tires B, C, and G at different temperatures.

| Young's Modulus - Frequency 10 Hz |                  |   |  |  |   |  |  |  |  |
|-----------------------------------|------------------|---|--|--|---|--|--|--|--|
| Sample                            | Temperature [°C] | <i>E'</i> [MPa]   | <i>E"</i> [MPa]  | TAN-D  | <i>E</i> *<br>[MPa]   |  |  |  |  |
| В                                 | -11.2            | 4.002   | 1.106  | 0.276  | 4.152   |  |  |  |  |
|                                   | -8.3             | 3.697   | 0.946  | 0.256  | 3.816   |  |  |  |  |
|                                   | -5.6             | 3.495   | 0.808  | 0.231  | 3.587   |  |  |  |  |
|                                   | -2.7             | 3.401   | 0.765  | 0.225  | 3.486   |  |  |  |  |
|                                   | 0.4              | 3.137   | 0.587  | 0.187  | 3.191   |  |  |  |  |
| С                                 | -11.7            | 5.12  | 1.205  | 0.235  | 5.26  |  |  |  |  |
|                                   | -8.4             | 4.916   | 1.044  | 0.212  | 5.025   |  |  |  |  |
|                                   | -5.3             | 4.556   | 0.839  | 0.184  | 4.633   |  |  |  |  |
|                                   | -2.3             | 4.197   | 0.771  | 0.184  | 4.268   |  |  |  |  |
|                                   | 0.6              | 4.153   | 0.762  | 0.184  | 4.222   |  |  |  |  |
| G                                 | -11.8            | 7.421   | 1.508  | 0.203  | 7.573   |  |  |  |  |
|                                   | -8.5             | 6.628   | 1.24   | 0.187  | 6.743   |  |  |  |  |
|                                   | -5.3             | 6.489   | 1.115  | 0.172  | 6.584   |  |  |  |  |
|                                   | -2.3             | 6.184   | 0.992  | 0.16   | 6.263   |  |  |  |  |
|                                   | 0.6              | 6.03  | 0.983  | 0.163  | 6.11  |  |  |  |  |
|                                   | Sample<br>B      | Sample [°C]  B -11.2 -8.3 -5.6 -2.7 0.4 C -11.7 -8.4 -5.3 -2.3 0.6 G -11.8 -8.5 -5.3 -2.3 | Sample         Temperature [°C]         E' [MPa]           B         -11.2         4.002           -8.3         3.697           -5.6         3.495           -2.7         3.401           0.4         3.137           C         -11.7         5.12           -8.4         4.916           -5.3         4.556           -2.3         4.197           0.6         4.153           G         -11.8         7.421           -8.5         6.628           -5.3         6.489           -2.3         6.184 | Sample         Temperature [°C]         E' [MPa]         E" [MPa]           B         -11.2         4.002         1.106           -8.3         3.697         0.946           -5.6         3.495         0.808           -2.7         3.401         0.765           0.4         3.137         0.587           C         -11.7         5.12         1.205           -8.4         4.916         1.044           -5.3         4.556         0.839           -2.3         4.197         0.771           0.6         4.153         0.762           G         -11.8         7.421         1.508           -8.5         6.628         1.24           -5.3         6.489         1.115           -2.3         6.184         0.992 | Sample         Temperature [°C]         E' [MPa]         E" [MPa]         TAN-D           B         -11.2         4.002         1.106         0.276           -8.3         3.697         0.946         0.256           -5.6         3.495         0.808         0.231           -2.7         3.401         0.765         0.225           0.4         3.137         0.587         0.187           C         -11.7         5.12         1.205         0.235           -8.4         4.916         1.044         0.212           -5.3         4.556         0.839         0.184           -2.3         4.197         0.771         0.184           G         -11.8         7.421         1.508         0.203           -8.5         6.628         1.24         0.187           -5.3         6.489         1.115         0.172           -5.3         6.184         0.992         0.16 |  |  |  |  |

tests with various camber angles and toe angles in the future, if needed.

For each combination from the DOE in <u>Table 3</u>, at least two tests were conducted and the average results of these tests are presented in this article.

### 4. Testing Setup

The tires considered in this study were run for 100 km before they were used for indoor testing at TMVS. They were also rotated diagonally every 25 km. All these tests were performed in three days before conducting the indoor tests. Eight thermocouples were mounted on each tire to collect the

**TABLE 3** DOE for the study of the effects of rubber compound on the tire performance on ice.

|  | Nominal load = 7 kN               | Nominal inflation pressure = 241 kPa<br>I (35 psi)                    |     |             |     |             |     |             |     |
|--|-----------------------------------|---|-----|-------------|-----|-------------|-----|-------------|-----|
|  |                                   | Level 1   |     | Level 2     |     | Level 3     |     | Level 4     |     |
|  | Tire type                         | SRTT  |     | Tire B      |     | Tire C      |     | Tire G      |     |
|  | Load [kN]                         | 4   | 5.6 | 4           | 5.6 | 4           | 5.6 | 4           | 5.6 |
|  | Inflation pressure [%]            | 60  | 80  | 60          | 80  | 60          | 80  | 60          | 80  |
|  | Tire temp [°C]                    | -10, -5, -1   |     | -10, -5, -1 |     | -10, -5, -1 |     | -10, -5, -1 |     |
|  | Ice temp [°C]                     | -10, -1   |     | -10, -1     |     | -10, -1     |     | -10, -1     |     |
|  | Slip ratio                        | 0%, 2%, 4%, 8%, 12%, 15%, 20%, 30%                                    |     |             |     |             |     |             |     |
|  | Free rolling                      | Free-rolling test performed for each case                             |     |             |     |             |     |             |     |
|  | Braking                           | Braking test performed for each case                                  |     |             |     |             |     |             |     |
|  | Pressure distribution measurement | Pressure at the contact patch measured for different cases of the DOE |     |             |     |             |     |             |     |

**FIGURE 2** Experimental setup at TMVS laboratory for testing tires on ice.



temperature changes at the contact patch. To have the tires at the desired temperature on the ice, the tires were cooled using the Thermotron system before conducting the tests. The terrain is hard and smooth ice that has been made by spraying a 2 mm height of water every 2 hours for several days until reaching the ice thickness of 8 cm. The static friction coefficient of the ice was checked and the ice surface was prepared frequently using several tools available in the lab to maintain the constant desired value  $(0.1 = \mu)$  for the friction coefficient. However, it is necessary to mention that this value was measured by the friction measurement tool for each test for consistency during the tests, but it is not accurate to say that this value is identical to the static friction coefficient of the tire on ice.

The Terramechanics Rig in the TMVS Lab at Virginia Tech, shown in Figure 2 has been used to conduct the indoor tests to study the effect of the tire tread rubber compounds. The rig has been designed to investigate tire performance under various operational conditions, such as different normal loads, inflation pressure, slip ratios, toe angles, and camber angles, for the tire in contact with various types of terrain conditions, such as ice and soil [20]. A clutch and a brake were added recently to the rig in order to expand its capabilities to study the tire performance under free-rolling and braking conditions [21].

The carriage motor provides a linear speed of around 6 cm/s in the longitudinal direction of the test surface, and the wheel motor applies a torque on the tire that enables the simulation of traction (positive torque) and braking (negative torque). Real braking conditions can be obtained using the brake system. Free rolling of the tire can be achieved by disengaging the clutch. Two air springs are used to apply a normal load on the tire with a precision of about 3%. A six-axis wheel measurement system from Kistler P650 force hub is used to collect the forces and the moments at the wheel, as well as the rotational speed of the hub and its angular orientation. The data is collected and processed using an LMS Test Lab package.

The slip ratio can be defined as indicated in <u>Equation (1)</u> [22] for the traction condition:

$$S = \frac{R_e \omega - V}{R_e \omega}$$
 Eq. (1)

where *S* is the slip ratio,  $\omega$  is the angular speed of the tire, *V* is the longitudinal speed of the carriage, and  $R_e$  is the effective rolling radius of the tire.

As was presented in [13], the ice surface preparation requires the following steps:

- 1. Laying the metal U-channels on the top level of the test chamber of the rig and placing two layers of thick plastic sheeting on top of the U-channels.
- 2. Placing a layer of insulation foam over the plastic tarp and covering it with another layer of plastic sheet.
- Rolling out the Custom Ice Rinks ice system (a tubular heat exchanger structure) on top of the plastic sheet.
- 4. Covering the connecting pipes with insulation and preparing the ice system by connecting the pipes to the outdoor chiller and the ice mat placed inside the rig. The ice mat helps make the ice and keeps the temperature of the ice at the desired value by circulating the cooled ethylene glycol in the plastic pipes/tubes.
- 5. The last step was spraying about 2 mm of water at a regular interval of 2 hours for 5 days to reach about 8 cm thickness of ice.
- 6. The ice surface was prepared using available tools in the lab to have the desired static friction coefficient.

The ice surface was prepared at a friction coefficient of 0.1 before each test. With the tire mounted on the test rig and the wheel motor on, a calibration of the Kistler sensor was performed next. After completion of the calibration step, the PiCPro software was set up in order to control the motors and, thus, the slip ratio.

These are the steps that have been completed for the experimental part of the study in summary:

- 1. Preparing and instrumenting the test tires (B, C, and G) with thermocouples.
- 2. Conducting the traction tests for various slip ratios of Tires B, C, and G from Sumitomo and Standard Reference Test Tire (SRTT), on ice with -10°C temperature. (Tire temperature = -10°C and -5°C)
- 3. Conducting the traction tests for various slip ratios of Tires B, C, and G from Sumitomo and SRTT, on ice with -1°C temperature. (Tire temperature = -1°C)
- 4. Conducting free-rolling tests for each case of the DOE.
- 5. Conducting braking tests for each case of the DOE.
- 6. Pressure distribution measurements under static loading, free-rolling, braking, and traction operations. The TekScan Pressure Pad 3150 with

2,288 sensels and a density of 1.4 sensels/cm² has been used to measure pressure distribution for pneumatic tires in different conditions. For the calibration and equilibration, an equilibrator has been used to apply a uniform and known load. After calibration, the desired normal load and the slip ratio are applied on the tire.

7. Data processing of the comparative study of the tires with different rubber compounds on ice.

# 5. Testing Results

The results obtained from the tests conducted according to the DOE table in order to study the effects of the rubber compounds on tire performance on ice have been presented in this section.

The experimental data that was obtained for this study can be divided into three categories:

- Data were obtained for the tire performance on ice using the Terramechanics Rig in the TMVS Lab that includes tire forces and moments in different directions.
- Data were measured and collected by thermocouples, and data loggers were mounted on the tires to monitor the tire temperature changes. The temperature changes of the tires and also the temperature of the room were measured and recorded during each test.
- 3. The last category of the data related to the pressure distribution data was measured using a pressure pad measurement tool. This data has been used as the main input for ATIIM2.0.

Part of the experimental results was collected by the LMS Test Lab software. To filter the existing noise in the system, a zero-phase low pass filter (finite impulse response (FIR)) has been used. The longitudinal force of the tire is the main performance parameter of this study. Using data collected for the longitudinal force of the tire, the drawbar pull coefficient and the equivalent friction coefficient have been calculated and plotted versus time for all cases in the DOE using MATLAB.

Tests have been conducted for the following three different conditions:

- 1. Traction, braking, and free-rolling tests for tires at -10°C in contact with ice at -10°C for 5.6 kN normal load and 193 kPa inflation pressure
- 2. Traction, braking, and free-rolling tests for tires at -5°C in contact with ice at -10°C for 5.6 kN normal load and 193 kPa inflation pressure
- 3. Traction, braking, and free-rolling tests for tires at -1°C in contact with ice at -1°C for 4 kN normal load and 144.8 kPa inflation pressure

The results for each condition are presented next.

# 5.1. Traction Tests for Tires with 193 kPa Pressure and 5.6 kN Normal Load with Tire Temperature around -10°C in Contact with Ice at -10°C

<u>Figure 3</u> shows the results of the traction tests. As can be seen, Tire B has better traction performance than Tires C and G under the given test conditions.

The normal load applied on the tire is controlled using a proportional valve and PID controller. To eliminate the effect of small variations in the normal load caused by the controller, the value of the drawbar pull coefficient has been obtained at all slip ratios considered.

Drawbar pull coefficient = 
$$\frac{F_X}{F_Z}$$
 Eq. (2)

where  $F_X$  is the longitudinal force measured by the Kistler sensor and Fz is the normal load on the tire measured by the Kistler sensor.

<u>Figure 4</u> shows the variation of drawbar pull coefficient for different slip ratios for Tires B, C, and G. Similar to the results for the longitudinal force, Tire B has higher traction than the other two Tires C and G under the given test conditions.

# 5.2. Traction Tests of Tires with 193 kPa Pressure and 5.6 kN Normal Load with Tire Temperature around -5°C in Contact with Ice at -10°C

To study the effects of tire temperature on tire performance, several tests were conducted for Tires B, C, and G with 193 kPa pressure and 5600 N normal load in contact with -10°C ice

**FIGURE 3** Longitudinal force for Tires B, C, and G with 193 kPa inflation pressure and 5.6 kN normal load in contact with ice at -10°C, ambient temperature of 10°C, tire temperature of -10°C, and ambient temperature of 10°C.

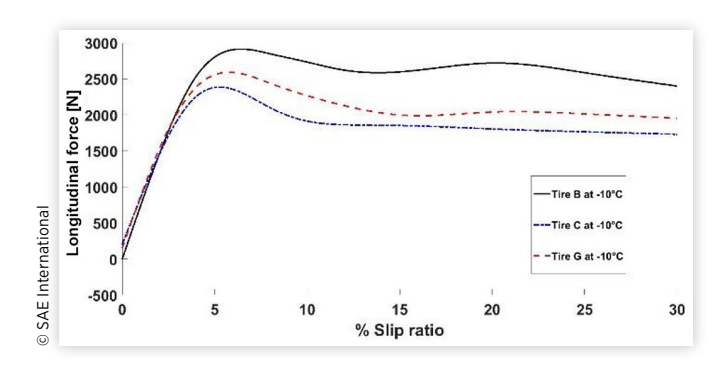


**FIGURE 4** Drawbar pull coefficient for Tires B, C, and G with 193 kPa inflation pressure and 5.6 kN normal load in contact with ice at -10°C, ambient temperature of 10°C, tire temperature of -10°C, and ambient temperature of 10°C.

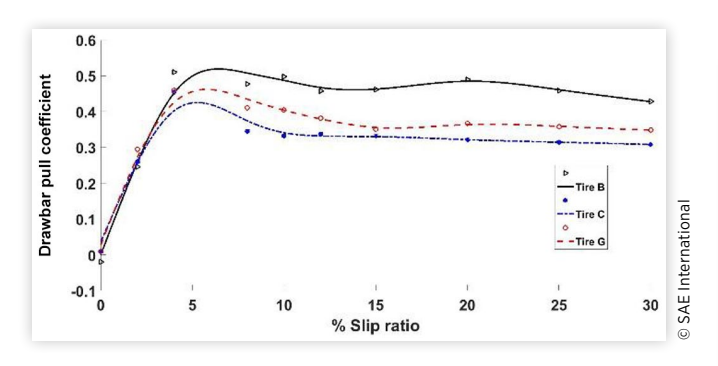
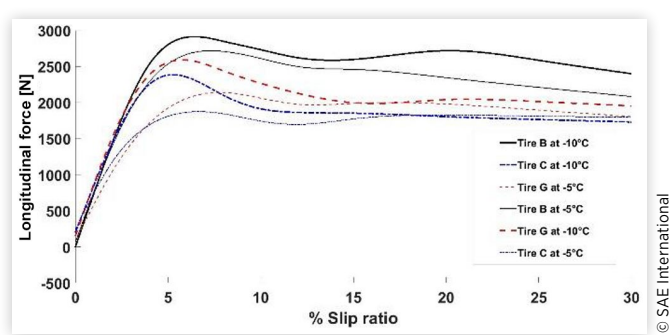


FIGURE 6 Comparative results for the longitudinal force for Tires B, C, and G with 193 kPa inflation pressure and 5.6 kN normal load in contact with ice at -10°C, ambient temperature of 10°C, and tire temperature at -10°C vs. tire temperature at -5°C.



for slip ratios of 0% to 30% when the tire temperature was -5°C and -10°C. <u>Figure 5</u> shows the drawbar pull coefficient force of Tires B, C, and G in the defined conditions.

<u>Figure 6</u> and <u>Figure 7</u> show the comparative results for longitudinal force and drawbar pull coefficient respectively for Tires B, C, and G. As can be seen in these figures, by increasing the tire temperature, the longitudinal force and the drawbar pull coefficient values decreased.

# 5.3. Traction Tests for Tires with 144.8 kPa Pressure and 4 kN Normal Load with Tire Temperature around -1°C in Contact with Ice at -1°C

<u>Figures 8</u> and <u>9</u> show the results for the traction tests conducted for Tires B, C and G. Five parameters have been

changed for the new set of the tests: tire temperature (from -10°C to -1°C), ice temperature (from -10°C to -1°C), ambient temperature (from 10°C to 12°C for Tires B and C and from 10°C to 15°C for Tire G), normal load (from 5.6 kN to 4 kN), and inflation pressure (from 193 to 144.8 kPa). As can be seen in Figures 6 and 7, similar to the previous results for the tires with 5.6 kN normal load, Tire B shows the highest traction for different slip ratios. To compare the results obtained for Tires B, C, and G with the results for the SRTT, the results for the longitudinal force for all these tires are presented in Figures 6 and 7.

As it can be seen from the results for the traction tests, Tire B exhibited a higher tractive force under all testing conditions. Based on these results one can determine which tire compound performs better without having to compare the performance of the tires at specific temperatures, as the ranking of the tire performance seems to be the same for all temperatures tested. However, the results are helpful in assessing the sensitivity of the magnitude of the tire forces with respect to the tire temperature.

**FIGURE 5** Drawbar pull coefficient for Tires B, C, and G with 193 kPa inflation pressure and 5.6 kN normal load in contact with ice at -10°C, ambient temperature of 10°C, tire temperature of -5°C, and ambient temperature of 10°C.

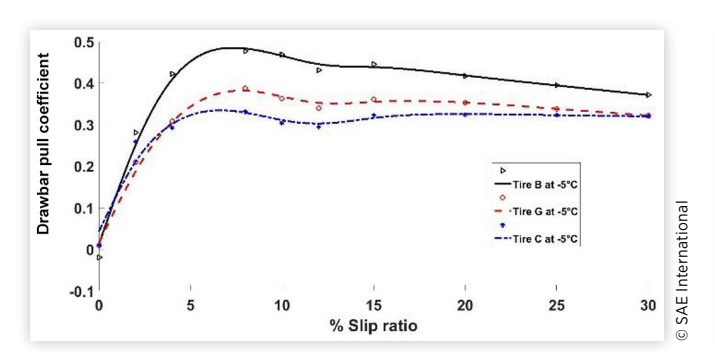


**FIGURE 7** Comparative results for drawbar pull coefficient for Tires B, C, and G with 193 kPa inflation pressure and 5.6 kN normal load in contact with ice at -10°C, ambient temperature of 10°C, and tire temperature at -10°C vs. tire temperature at -5°C.

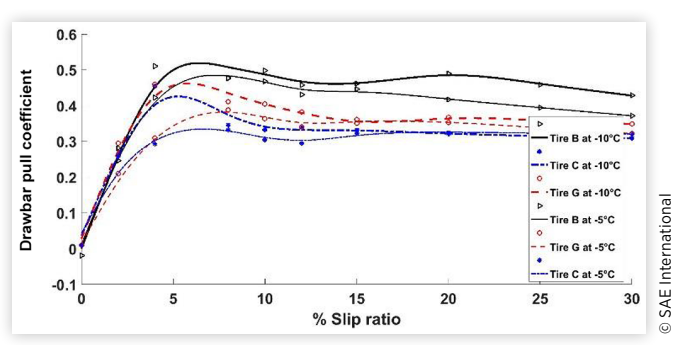
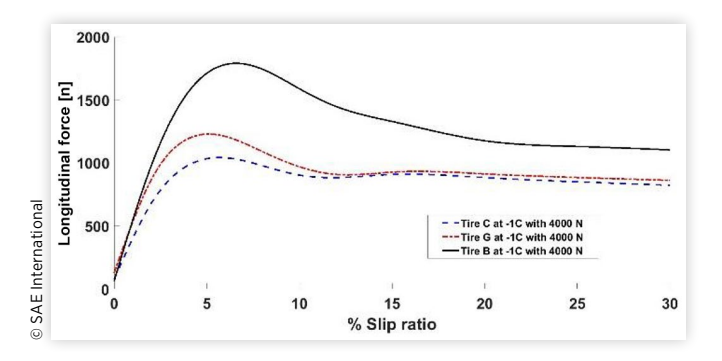


FIGURE 8 Longitudinal force for Tires B, C, and G with 144.8 kPa inflation pressure and 4 kN normal load in contact with ice at -1°C, tire temperature of -1°C, and ambient temperature of 10°C for Tire B and Tire C and 15°C for Tire G.



### 5.4. Results for Free-Rolling Tests of Tires B, C, and G

<u>Figures 10</u> and <u>11</u> show the longitudinal force of the tire when it is in free rolling. For the free-rolling condition, there is no applied torque on the wheel so the only force in the longitudinal direction is the resistive force (rolling resistance and friction force).

The results for the dynamic friction force for all the tires at -10°C with 5.6 kN normal load and 193 kPa inflation pressure are shown in Figure 11. For these tests, the Kistler sensor has been calibrated when the tire was rotating in a free-rolling condition on the ice surface. By calibrating the Kistler sensor this way, a significant portion of the resistive force has been removed from the measured longitudinal force. While this is desired for the traction portion of the study, as the remaining longitudinal force is then representative of the tractive force, it affects the accuracy of estimating the total resistive force in free rolling.

**FIGURE 9** Drawbar pull coefficient for Tires B, C, and G with 144.8 kPa inflation pressure and 4 kN normal load in contact with ice at -1°C, tire temperature of -1°C, and ambient temperature of 10°C for Tire B and Tire C and 15°C for Tire G.

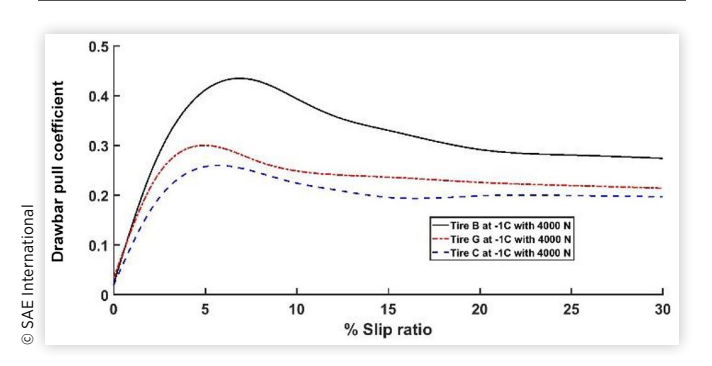
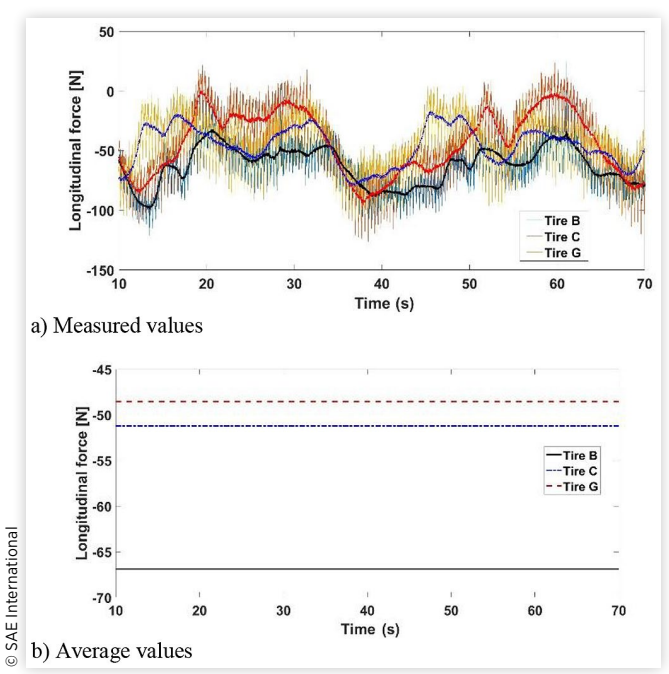


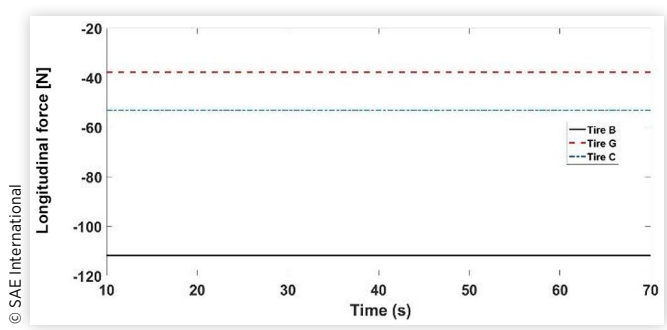
FIGURE 10 (a) Longitudinal force (friction force) for Tires B, C, and G with 144.8 kPa inflation pressure and 4 kN normal load in contact with ice at -1°C, ambient temperature of 10°C for Tires B and C and 15°C for Tire G, and tire temperature of -1°C. (b) Average value of the friction force.



The small variation in the longitudinal force during the test could be due to small differences in the ice surface friction and the applied normal load.

The small values obtained for the resistive force in average values, <u>Figures 10</u> and <u>11</u>, are caused by the difference in the ice surface characteristics for different runs. This means that calibrating the Kistler system on the ice surface cannot remove all the resistive force from the measured longitudinal force. As presented in <u>Figures 10</u> and <u>11</u>, the remained resistive force for Tire B is higher than Tires C and G for all cases of the

FIGURE 11 Average value of the friction force for Tires B, C, and G with 193 kPa inflation pressure and 5.6 kN normal load in contact with ice at -10°C, ambient temperature of 10°C, and tire temperature of -10°C.



DOE. Tire C has the second-largest resistive force value in all cases studied.

In addition, as can be seen from the presented figures, larger friction forces resulted when the tire was cooler and also when the applied normal load was higher. More research is still needed to fully understand the effects of each parameter separately.

### 5.5. Results for Braking Performance of Tires B, C, and G

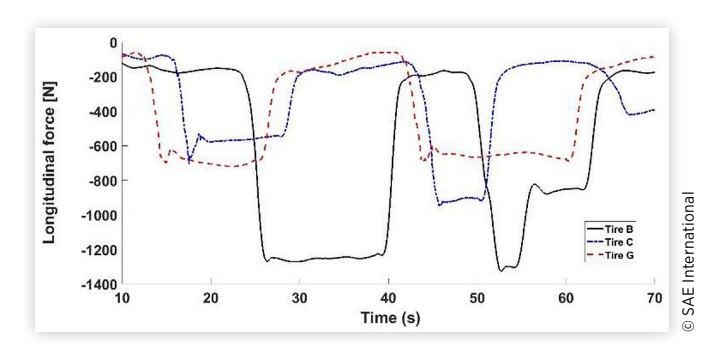
In addition to the tests for free rolling, several tests were conducted for the braking performance of the tires. <u>Figure 12</u> shows the results for the braking performance of the tire for the system calibrated with the tire in contact with the ice.

<u>Figure 13</u> shows the results for the braking performance of Tire B for the system calibrated when the tire was not in contact with the ice.

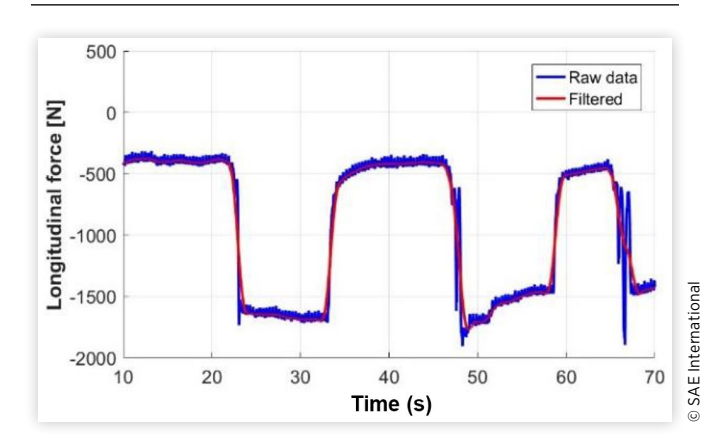
As the longitudinal force of the tire for the braking condition is highly dependent on the applied braking force, it is better to not use the magnitude of the maximum resistive force to compare the tire performance. However, the general trend can be useful. For example, in all the cases we have a pick value at the beginning of applying the braking force.

Figure 12 includes two modes of driving: free rolling and braking. The horizontal line at the beginning of each graph (values below 200 N) shows the value of the tire friction force in free rolling. After that, the sharp increase in the absolute value of the friction force is due to the applied braking force. As can be seen from the free-rolling part of the graph, the magnitude of the absolute value of Tire B friction force is higher than for Tire C, which in turn is higher than for Tire G. This order coincides with the one obtained in Section 5.4 for the free-rolling condition.

**FIGURE 12** Results of the braking tests for Tires B, C, and G with 144.8 kPa inflation pressure and 4 kN normal load in contact with ice at -1°C, ambient temperature of 10°C for Tires B and C and 15°C for Tire G, and tire temperature of -1°C. The rig was calibrated when the tire was in contact with the ice surface.



**FIGURE 13** Results of the braking tests for Tire B with 193 kPa inflation pressure and 5.6 kN normal load in contact with ice at -10°C, ambient temperature of 10°C, and tire temperature of -10°C. The rig was calibrated when the tire was not in contact with the ice surface.



### 6. Simulation

When studying the tire-ice interaction, it is important to consider the parameters that affect the magnitude of the friction coefficient. When a tire is in contact with ice, one of these parameters is the amount of water created at the contact patch. As the nature of the friction coefficient will change from dry friction to a combination of viscous and dry friction, the magnitude of the friction coefficient will decrease by increasing the area of the wet regions at the contact patch. To compare the performance of the tires with different rubber compounds, it is important to study the factors that affect the friction coefficient at the contact area. In this study, using an in-house developed tire-ice model, ATIIM2.0 [23, 24], the height of the water film created at the contact patch has been obtained for the tires in our cases of study. All other parameters except for the material properties of the rubber compounds were kept constant during the tests and for the modeling for each tire.

To use ATIIM2.0 in order to obtain the height of the water film generated at the contact patch, several input data are required: 1. Material properties of the tire tread rubber compounds (Young's modulus, specific heat, density, roughness parameters, and thermal conductivity). 2. Operational parameters (applied normal load, inflation pressure of the tire, static friction coefficient, temperature of the ice and tire, and slip ratio). 3. Data collected by the experiment are pressure distributions at the contact patch and the temperature changes at the contact area.

To collect the pressure distribution data, several tests were conducted at TMVS using the TekScan Pressure Pad 3150. The normal load of 4 kN was applied on each of the tires (B, C, and G). The inflation pressure was set at 144.8 kPa. The ice and tire temperatures were kept constant at -1°C. For traction condition, the slip ratio was set at several values from 2% to 30%.

<u>Figures 14</u> through <u>19</u> show the data collected for pressure pad distribution at the contact area for Tire B, C,

**FIGURE 14** Pressure distribution for Tires B with 2% slip ratio with 144.8 kPa inflation pressure and 4 kN normal load in contact with ice at -1°C and tire temperature of -1°C.

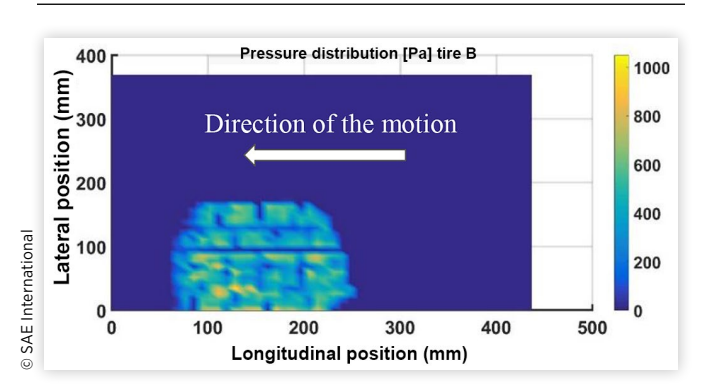


**FIGURE 17** Pressure distribution for Tire B with 10% slip ratio with 144.8 kPa inflation pressure and 4 kN normal load in contact with ice at -1°C and tire temperature of -1°C.

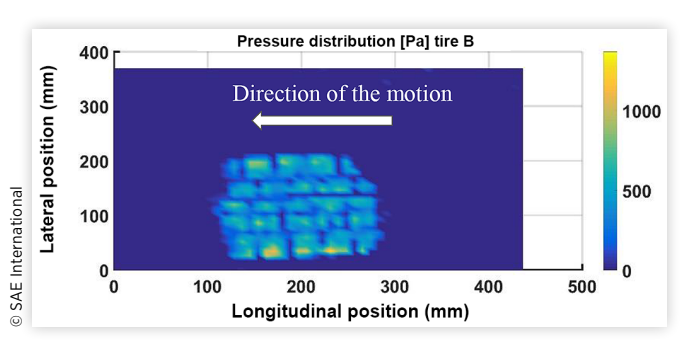


**FIGURE 15** Pressure distribution for Tire C with 2% slip ratio with 144.8 kPa inflation pressure and 4 kN normal load in contact with ice at -1°C and tire temperature of -1°C.

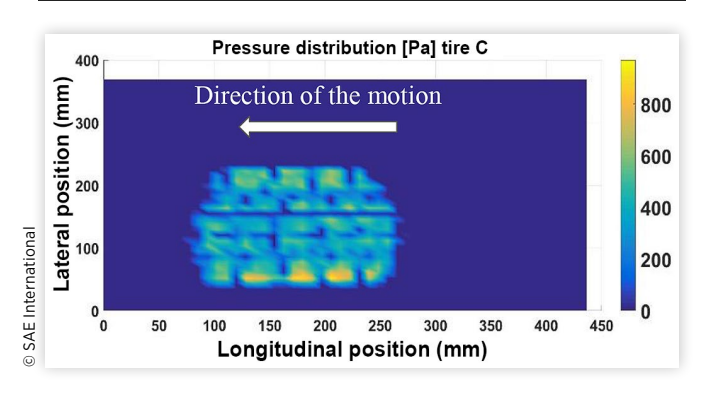


**FIGURE 18** Pressure distribution for Tire C with 10% slip ratio with 144.8 kPa inflation pressure and 4 kN normal load in contact with ice at -1°C and tire temperature of -1°C.

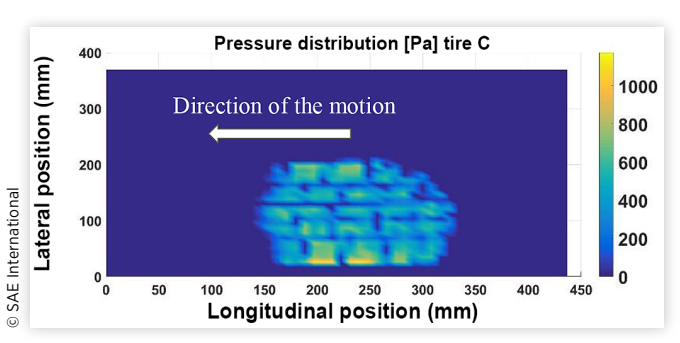


**FIGURE 16** Pressure distribution for Tire G with 2% slip ratio with 144.8 kPa inflation pressure and 4 kN normal load in contact with ice at -1°C and tire temperature of -1°C.

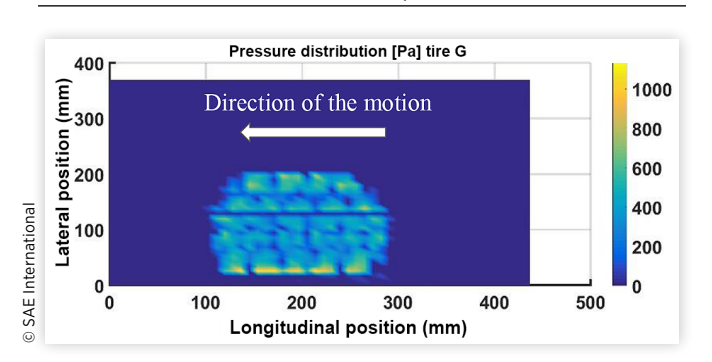


**FIGURE 19** Pressure distribution for Tire G with 10% slip ratio with 144.8 kPa inflation pressure and 4 kN normal load in contact with ice at -1°C and tire temperature of -1°C.

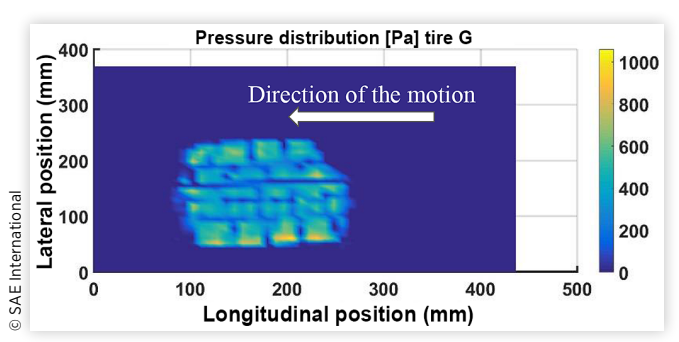
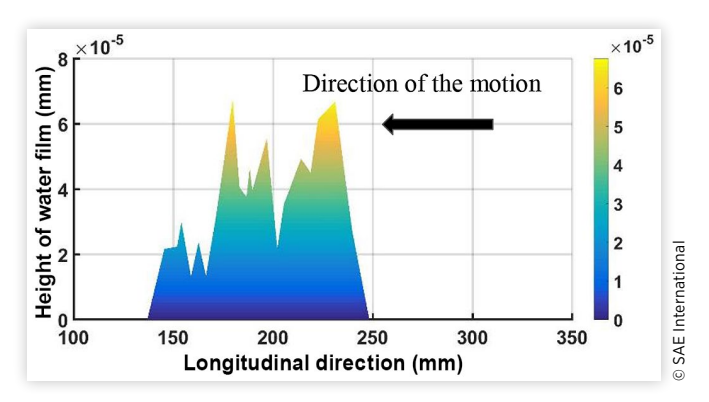


FIGURE 20 Distribution of height of the water film for Tire B with 2% slip ratio with 144.8 kPa inflation pressure and 4 kN normal load in contact with ice at -1°C and tire temperature of -1°C.

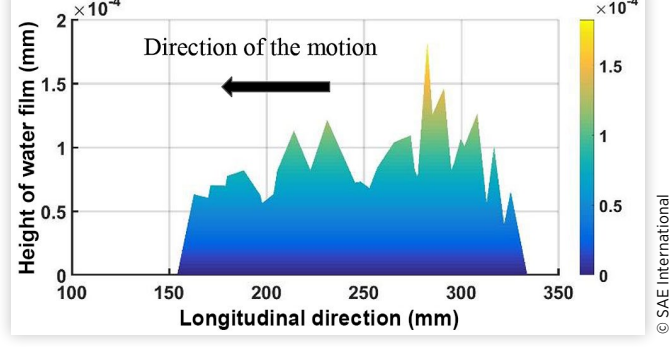


temperature of -1°C.  $\times 10^{-4}$ ×10<sup>-4</sup> (mm) Direction of the motion 1.5

FIGURE 22 Distribution of height of the water film for

4 kN normal load in contact with ice at -1°C and tire

Tire B with 8% slip ratio with 144.8 kPa inflation pressure and



and G at 2% and 10% slip ratio. As seen in these figures, for all three tires, by increasing the slip ratio, the shape of the contact area is deforming and the pressure distribution is changing towards having higher pressure at the leading edge of the contact area.

As it is difficult to compare the performance of the tires using only the data collected by the pressure pad, the ATTIM2.0 has been used to obtain the height of the water film generated at the contact patch. Considering the important role of this parameter in the magnitude of the friction coefficient, evaluating the height of the water film for each tire will help us compare the performance of the tires. Figures 20 through 25 show the distribution of the height of the water film generated at the contact patch along a longitudinal direction for Tire B with 4 kN normal load and 144.8 kPa inflation pressure at slip ratio from 2% to 30%. As can be seen from the presented figures for the height of the water film, there is an increasing trend for the magnitude of the height of the water film from the leading edge to the trailing edge for all slip ratios. In addition, an increase in the height

of the water film can be observed when the slip ratio increases. By increasing the amount of water at the contact patch, the friction coefficient decreases as the contact area converts from a dry region to a combination of wet and dry regions.

To compare the performance of all three tires, the values of the height of the water film have been obtained for different slip ratios using ATIIM2.0. Figures 26 through 28 have been presented to compare the results for the height of the water film for Tires B, C, and G at 8% slip ratio. As has been shown, the height of the water film generated at the contact patch is higher for Tire G. Tire C has the secondhighest height of water film with an average value of 7.8e-05 mm in comparison with Tire B with the average value of 6.9e-05 mm height of water film. According to Equation (3), which shows the calculation of the viscous friction coefficient in the contact area of the tire and ice, by increasing the height of the water film, the friction coefficient decreases. That means that Tire B with the lowest height of water film has the highest friction coefficient

FIGURE 21 Distribution of height of the water film for Tire B with 4% slip ratio with 144.8 kPa inflation pressure and 4 kN normal load in contact with ice at -1°C and tire temperature of -1°C.

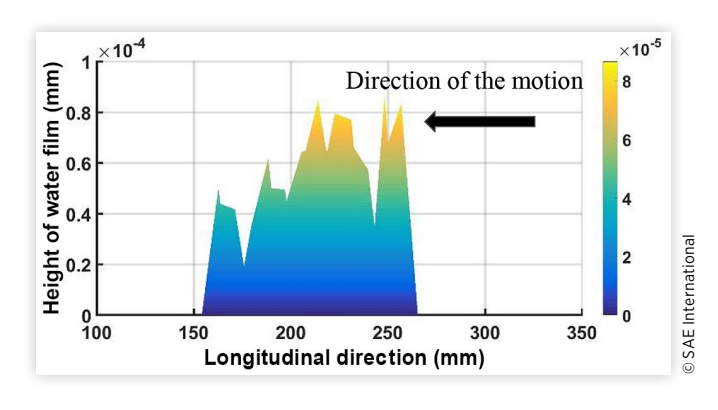


FIGURE 23 Distribution of height of the water film for Tire B with 10% slip ratio with 144.8 kPa inflation pressure and 4 kN normal load in contact with ice at -1°C and tire temperature of -1°C.

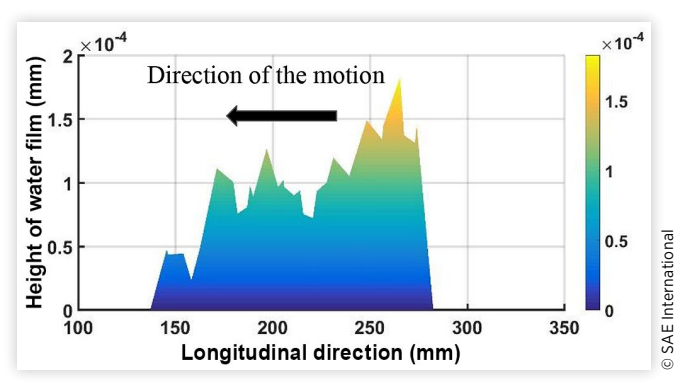
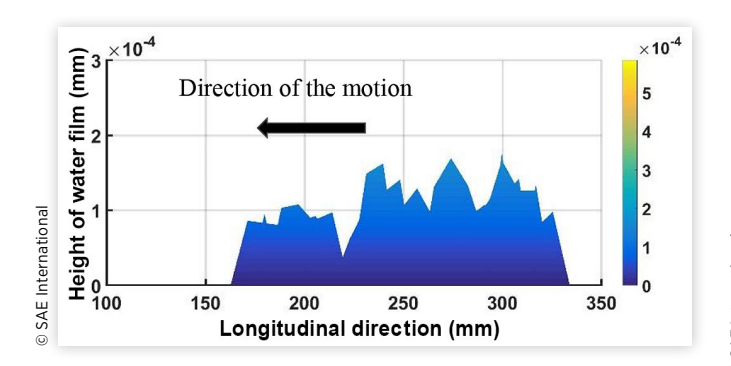


FIGURE 24 Distribution of height of the water film for Tire B with 12% slip ratio with 144.8 kPa inflation pressure and 4 kN normal load in contact with ice at -1°C and tire temperature of -1°C.



among all three tires. The results obtained by ATIIM2.0 coincide with the results obtained experimentally.

$$\mu = \frac{\eta v \kappa}{hP},$$
 Eq. (3)

where h is the height of water film, P is the applied pressure on the contact area, v is sliding velocity,  $\eta$  is the viscosity of the ice, and  $\kappa$  is the relative real contact area.

### 7. Conclusion

To study the effect of the rubber compound on tire performance on ice, two approaches were considered in this article: experimental approach and simulation approach.

To compare the performance of the tires with different rubber compounds experimentally, several tests have been conducted for three similar tires but with different material properties of the rubber compounds. The tests were conducted for free-rolling, braking, and traction conditions for different

FIGURE 25 Distribution of height of the water film for Tire B with 15% slip ratio with 144.8 kPa inflation pressure and 4 kN normal load in contact with ice at -1°C and tire temperature of -1°C.

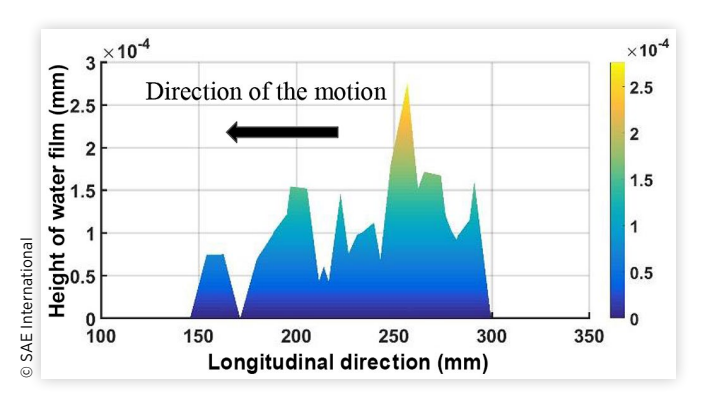
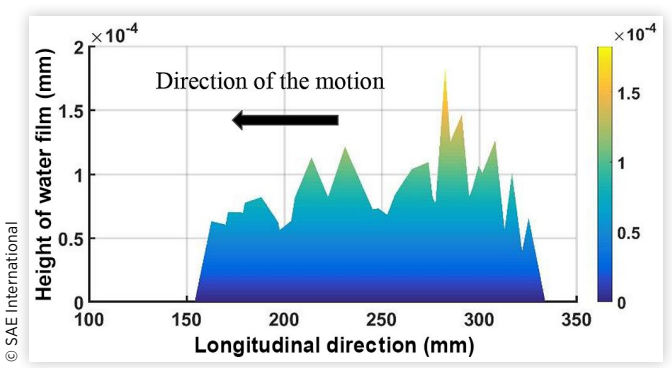


FIGURE 26 Distribution of height of the water film for Tire B with 8% slip ratio with 144.8 kPa inflation pressure and 4 kN normal load in contact with ice at -1°C and tire temperature of -1°C.



normal loads, inflation pressure, and ice and tire temperatures. The comparative results have been presented for all three tires under different test conditions.

From the presented results, tires at lower temperatures show higher tractive performance. Increasing the tire temperature causes a water film on the ice, and thus it decreases the friction coefficient. Furthermore, it has been found that the best tractive performance is obtained at higher slip ratio values when the tire is warmer. For example, it can be seen that the pick value of the longitudinal force for 5.6 kN normal load for tires at -10°C happened around 5% slip ratio; however, the pick value of the longitudinal force for the tires at -5°C happened around 8% slip ratio. The longitudinal force increases until it reaches a maximum value, and then it decreases until it almost plateaus to a constant value.

From the presented results, the best, under all testing conditions, was obtained for Tire B, which had the smallest value of Young's modulus and specific heat parameter. The results also show that the ranking order for Tires B, C, and G is not dependent on the testing conditions. However, the results indicated the sensitivity of the magnitude of the tire

FIGURE 27 Distribution of height of the water film for Tire C with 8% slip ratio with 144.8 kPa inflation pressure and 4 kN normal load in contact with ice at -1°C and tire temperature of -1°C.

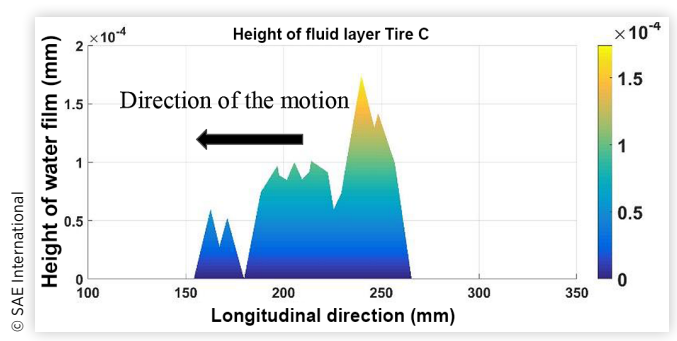
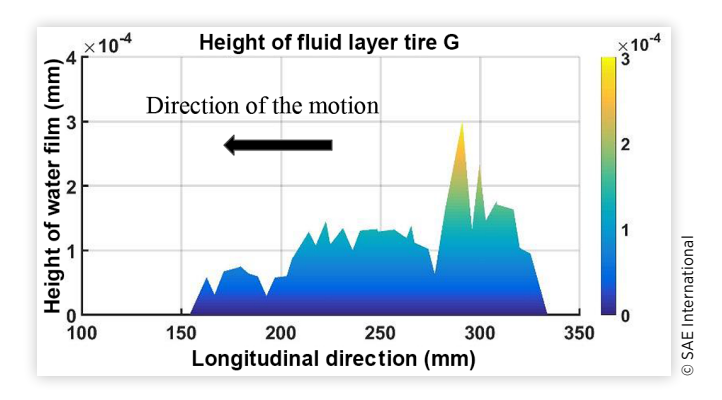


FIGURE 28 Distribution of height of the water film for Tire G with 8% slip ratio with 144.8 kPa inflation pressure and 4 kN normal load in contact with ice at -1°C and tire temperature of -1°C.



forces with respect to the tire temperature, as the tire temperature affects the rubber compounds properties. The results for free-rolling performance show that Tire B has the largest absolute value of the resistive force among the tires tested. Tire C has the next largest resistive force. These results show the sensitivity of the magnitude of the friction force with respect to the rubber physical and thermal parameters, such as Young's modulus and specific heat.

In order to study the effect of different rubber compounds using the simulation method, a semi-analytical tire-ice model has been developed. The model was used to predict the height of the water film generated at the contact patch. The results were obtained using the simulations presented in this study. The results show that the amount of water generated at the contact area increases by increasing the slip ratio. It is also shown that the height of the water film is higher in the trailing edge of the contact patch. According to the simulation results, Tire B generates the lowest height of the water film among all three tires. This is why this tire has the highest friction coefficient. Tire C has the second-lowest height of water film. The results coincide with the experimentally obtained results.

Further investigation is required to improve the correlations between rubber compound properties and tire performance under traction, braking, and free rolling.

### **Contact Information**

Hoda Mousavi hoda13@vt.edu

Corina Sandu csandu@vt.edu

### **Acknowledgments**

The authors would like to thank TMVS lab for the testing facilities used in this study and the support of the NSF I/UCRC Center for Tire Research (CenTiRe) who partially funded this

work. The authors also would like to thank Mr. Mehran Shams and Mr. Mohit Nitin Shenvi for their help in conducting the tests for the experimental study.

### References

- Bhoopalam, A.K., Sandu, C., and Taheri, S., "A Tire-Ice Model (TIM) for Traction Estimation," *Journal of Terramechanics* 66:1-2, 2016, <a href="https://doi.org/10.1016/j.jterra.2016.02.003">https://doi.org/10.1016/j.jterra.2016.02.003</a>.
- Bhoopalam, A.K., Sandu, C., and Taheri, S., "Experimental Investigation of Pneumatic Tire Performance on Ice: Part 1-Indoor Study," *Journal of Terramechanics* 60:43-54, 2015, https://doi.org/10.1016/j.jterra.2015.02.006.
- He, R., Mousavi, H., Sandu, C., and Osorio, E.J., "Modeling and Experimental Study of Tire Motion Resistance on Soft Soil," in *Proceedings of the ISTVS 15th European-African* Regional Conference, in Prague, Czech Republic, September 9-11, 2019.
- Esmaeeli, R., Aliniagerdroudbari, H., Hashemi, S.R., Jbr, C. et al., "Designing a New Dynamic Mechanical Analysis (DMA) System for Testing Viscoelastic Materials at High Frequencies," *Modelling and Simulation in Engineering*, 2019, https://doi.org/10.1155/2019/7026267.
- Isitman, N.A., Kriston, A., and Fülöp, T., "Role of Rubber Stiffness and Surface Roughness in the Tribological Performance on Ice," *Tribology Transactions* 61(2):295-303, 2018, https://doi.org/10.1080/10402004.2017.1319002.
- Hemmette, S., Kasuya, M., Lecadre, F. et al., "Viscoelasticity of Rubber-Ice Interfaces under Shear Studied Using Low-Temperature Surface Forces Apparatus," *Tribology Letters* 67:74, 2019, <a href="https://doi.org/10.1007/s11249-019-1187-2">https://doi.org/10.1007/s11249-019-1187-2</a>.
- Zhang, Y., Gao, J., and Li, Q., "Experimental Study on Friction Coefficients between Tire Tread Rubber and Ice," AIP Advances 8(7), 2018, https://doi.org/10.1063/1.5041049.
- 8. Esmaeeli, R., Nazari, A., Aliniagerdroudbari, H., Hashemi, S.R. et al., "Heat Built up during Dynamic Mechanical Analysis (DMA) Testing of Rubber Specimens," in ASME International Mechanical Engineering Congress and Exposition, Proceedings (IMECE) 9: 61DUMM0Y, 2018, https://doi.org/10.1115/IMECE2018-88627.
- Gao, J., Zhang, Y., Du, Y., and Li, Q., "Optimization of the Tire Ice Traction Using Combined Levenberg-Marquardt (LM) Algorithm and Neural Network," *Journal of the* Brazilian Society of Mechanical Sciences and Engineering 41(1):1-8, 2019, https://doi.org/10.1007/s40430-018-1545-2.
- He, R., Sandu, C., and Osorio, J.E., "Investigating the Parameterization of Magic Formula Tire Model Using Data from Dynamic Tire-Soil Tests," in *Proceedings eof the 10th* Asia-Pacific Conference of the ISTVS, Japan, 2018, 1-18.
- 11. Liang, C., Ji, L., Mousavi, H., and Sandu, C. "EsStress," SIAR International Congress of Automotive and Transport Engineering: Science and Management of Automotive and Transportation Engineering, Springer, Cham, 138-152, 2019, http://doi.org/10.1007/978-3-030-32564-0\_17.

- 12. Mashhadi, B., Mousavi, H., and Montazeri, M., "Obtaining Relations between the Magic Formula Coefficients and Tire Physical Properties," *International Journal of Automotive Engineering* 5(1):911-922, 2015.
- 13. Mousavi, H., Shenvi, M.N., and Sandu, C., "Experimental Study for Free Rolling of Tire on Ice," presented at in ASME 2019 International Design Engineering Technical Conferences and Computers and Information in Engineering Conference IDETC/CIE 2019, 1-11, 2019, http://doi.org/10.1115/DETC2019-97846.
- 14. Ivanovic, V., Deur, J., Kostelac, M., Herold, Z. et al., "Experimental Identification of Dynamic Tire Friction Potential on Ice Surfaces," *Vehicle System Dynamics* 44(Suppl. 1):93-103, 2006, <a href="https://doi.org/10.1080/00423110600869230">https://doi.org/10.1080/00423110600869230</a>.
- 15. Lasse, M. and Tikanmäki, M., "Modeling the Friction of Ice," *Cold Regions Science and Technology* 102:84-93, 2014, <a href="https://doi.org/10.1016/j.coldregions.2014.03.002">https://doi.org/10.1016/j.coldregions.2014.03.002</a>.
- 16. Gießler, M., Gauterin, F., Wiese, K., and Wies, B., "Influence of Friction Heat on Tire Traction on Ice and Snow," *Tire Science and Technology* 38(1):4-23, 2010.
- Wiese, K., Thiemo, M.K., Reinhard, M., and Burkhard, W., "An Analytical Thermodynamic Approach to Friction of Rubber on Ice," *Tire Science and Technology* 40(2):124-150, 2012.

- Roberts, A.D., "Rubber-Ice Adhesion and Friction," *The Journal of Adhesion* 13(1):77-86, 1981, <a href="https://doi.org/10.1080/00218468108073176">https://doi.org/10.1080/00218468108073176</a>.
- 19. Polymer Database, "Polymer Properties Database," <a href="http://polymerdatabase.com/polymer">http://polymerdatabase.com/polymer</a>, accessed March 2020.
- Sandu, C., Taylor, B., Biggans, J., and Ahmadian, M., "Building an Infrastructure for Indoor Terramechanics Studies: The Development of a Terramechanics Rig at Virginia Tech.," in *Proceedings of 16th ISTVS International* Conference, Italy, 2008, 177-185.
- 21. Khan, A.K. and Sandu, C., "Design and Manufacturing of a Clutch and Brake System for Indoor Tire Testing," *Proceedings of the ASME Design Engineering Technical Conference* 3, 2017, https://doi.org/10.1115/DETC2017-67872.
- He, R., Shenvi, M.N., Mousavi, H., Sandu, C. et al. Updates of International Society for Terrain-Vehicle Systems Standards," Paper No. 30, in *Proceedings of the 15th ISTVS European-*African Regional Conference, Czech Republic, 4405, 2019, 1-91.
- 23. Mousavi, H. and Sandu, C., "Tire-Ice Model Development for the Simulation of Rubber Compounds Effect on Tire Performance," *J. Terramechanics*, PII: S0022-4898(20)30051-3, 2020, https://doi.org/10.1016/j.jterra.2020.06.00.
- 24. Mousavi, H. and Sandu, C., "Sensitivity Analysis of Tire-Ice Friction Coefficient as Affected by Tire Rubber Compound Properties," *J. Terramechanics*, 2020.

<sup>© 2020</sup> SAE International. All rights reserved. No part of this publication may be reproduced, stored in a retrieval system, or transmitted, in any form or by any means, electronic, mechanical, photocopying, recording, or otherwise, without the prior written permission of SAE International.

 $Downloaded \ from \ SAE \ International \ by \ Corina \ Sandu, \ Tuesday, \ January \ 05, 2021$